

# Brocaeloids A–C, 4-Oxoquinoline and Indole Alkaloids with C-2 Reversed Prenylation from the Mangrove-Derived Endophytic Fungus *Penicillium brocae*

Peng Zhang,<sup>[a,b]†</sup> Ling-Hong Meng,<sup>[a,b]†</sup> Attila Mándi,<sup>[c]</sup> Tibor Kurtán,<sup>\*[c]</sup> Xiao-Ming Li,<sup>[a]</sup> Yang Liu,<sup>[a,b]</sup> Xin Li,<sup>[a,b]</sup> Chun-Shun Li,<sup>[a]</sup> and Bin-Gui Wang<sup>\*[a]</sup>

Dedicated to Professor Dr. Sándor Antus on the occasion of his 70th birthday

**Keywords:** Natural products / Alkaloids / Circular dichroism / Density functional calculations

Three new alkaloids, brocaeloids A–C (**1–3**), containing C-2 reversed prenylation, were isolated from cultures of *Penicillium brocae* MA-192, an endophytic fungus obtained from the fresh leaves of the marine mangrove plant *Avicennia marina*. Their structures were determined on the basis of 1D and 2D NMR spectroscopy as well as by high-resolution mass spectrometry. The absolute configuration of brocaeloid A (**1**) was established by gas-phase and solution conformational analysis and TDDFT-ECD calculations, which revealed that the fused hetero-ring adopted *M*-helicity conformation with axial orientation of the C-2 and C-3 substituents. The correct

assignment of the hetero-ring conformation was found to be crucial in determining the relative and absolute configuration. Based on ECD calculations, the helicity of the 2,3-dihydroquinoline-4(1*H*)-one chromophore was correlated with the characteristic ECD transitions, and the resultant helicity rule was found to coincide with that of the chroman-4-one chromophore. X-ray single-crystal analysis of **1** by Cu- $K_{\alpha}$  radiation also confirmed the result of the stereochemical analysis obtained from ECD calculations. Brocaeloid B (**2**) showed lethality against brine shrimp (*Artemia salina*) with an LD<sub>50</sub> value of 36.7  $\mu$ M.

## Introduction

Marine-derived fungi are an important source of secondary metabolites that can possess both unique structure and potent pharmaceutical activity.<sup>[1]</sup> In recent years, an increasing number of bioactive natural products have been isolated from fungi associated with mangrove plants and their rhizospheric soils.<sup>[2]</sup> Our previous investigation of mangrove-derived endophytic fungi has resulted in the isolation and identification of a number of structurally unique and biological active secondary metabolites.<sup>[3–7]</sup> As a continuation of our investigations on the characterization of new bioactive secondary metabolites from marine-derived endophytes, three new alkaloids, brocaeloids A–C (**1–3**), which contain C-2-reversed prenylation in the molecules (Figure 1), were isolated and identified from *Penicillium brocae* MA-192, an endophytic fungus obtained from the

fresh leaves of marine mangrove plant *Avicennia marina*. Herein, we report the isolation, structure elucidation, absolute configuration assignment, and biological activity of these compounds.

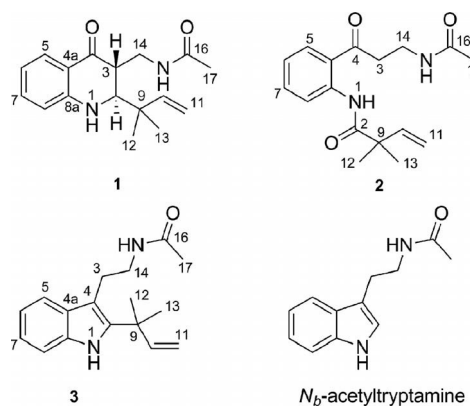


Figure 1. Chemical structures of isolated compounds **1–3** and the reference compound *N<sub>b</sub>*-acetyltryptamine.

## Results and Discussion

The ethyl acetate (EtOAc) soluble extract of *P. brocae* MA-192 was subjected to silica gel vacuum liquid chromatography (VLC) and was further purified by a com-

[a] Key Laboratory of Experimental Marine Biology, Institute of Oceanology, Chinese Academy of Sciences, Nanhai Road 7, Qingdao 266071, P. R. China  
E-mail: wangbg@ms.qdio.ac.cn

[b] University of Chinese Academy of Sciences, Yuquan Road 19A, Beijing 100049, P. R. China

[c] Department of Organic Chemistry, University of Debrecen, POB 20, 4010 Debrecen, Hungary  
E-mail: kurtan.tibor@science.unideb.hu  
[http://szerves.science.unideb.hu/eng/html/kurtan\\_tibor.html](http://szerves.science.unideb.hu/eng/html/kurtan_tibor.html)

† P. Z. and L. H. M. contributed equally to this work.

Supporting information for this article is available on the WWW under <http://dx.doi.org/10.1002/ejoc.201400067>.

## FULL PAPER

bination of column chromatography (CC) on silica gel, Sephadex LH-20, Lobar LiChroprep RP-18, and semipreparative HPLC to furnish three new compounds **1–3**.

56 Compound **1** was initially obtained as a light-yellow amorphous solid. Its molecular formula  $C_{17}H_{22}O_2N_2$  was established on the basis of the HRMS (ESI) ion at  $m/z$  287.1755  $[M + H]^+$  (calcd. for  $C_{17}H_{23}O_2N_2^+$ , 287.1754), indicating eight degrees of unsaturation. In the  $^1H$  NMR spectrum (Table 1), four aromatic signals resonating at  $\delta_H = 7.53$  (d,  $J = 7.8$  Hz, 5-H), 6.51 (t,  $J = 7.8$  Hz, 6-H), 7.24 (t,  $J = 7.8$  Hz, 7-H), and 6.81 ppm (d,  $J = 7.8$  Hz, 8-H), indicated the presence of a 1,2-disubstituted benzene system, which was supported by the corresponding COSY correlations as shown in Figure 2. A total of 17 carbon atoms including three methyls, two methylenes (one nitrogenated  $sp^3$  and one terminal  $sp^2$ ), seven methines (one nitrogenated  $sp^3$  and five  $sp^2$ ), and five quaternary (one amide and one ketone) carbon signals were observed in the  $^{13}C$  NMR and DEPT spectra (Table 1). The complete NMR assignments and connectivity of **1** were further determined by analysis of the 2D NMR spectroscopic data. The observed COSY correlations between N1-H and 2-H and between 10-H and  $CH_2$ -11 in the COSY spectrum, as well as HMBC correlations from the methyl protons  $CH_3$ -12 and  $CH_3$ -13 to C-2, C-9, and C-10 (Figure 2) indicated the presence of a  $-NHCHC(CH_3)_2CH=CH_2-$  fragment in the structure of **1**. The clear HMBC cross-peaks from 2-H to the nitrogenated aromatic carbon C-8a revealed that the above fragment should connect to the benzene ring through NH-1 at C-8a. Additionally, COSY correlations between NH-15 to  $CH_2$ -14 and between  $CH_2$ -14 to 3-H as well as the HMBC correlation from 3-H to the ketone carbonyl group C-4 established the fragment  $COCHCH_2NH-$ . The HMBC correlation from the aromatic proton 5-H to the C-4 ketone carbonyl established the connection of this fragment to C-

4a. The HMBC cross-peak from the acetyl methyl protons  $CH_3$ -17 to the carbonyl group C-16 implied the existence of an acetyl group. Combined with the characteristic signals, the acetyl group was deduced to be connected with N-15 to form the acetamide moiety. The fragments deduced above including a benzene ring, a double bond, and two carbonyl groups accounted seven out of eight degrees of unsaturation, suggesting the presence of an additional fused 2,3-dihydropyridin ring in **1**. The COSY correlation between 2-H and 3-H supported the presence of a 2,3-dihydroquinoline-4(1*H*)-one moiety, which was further confirmed by the HMBC correlations from 2-H to C-3, C-4, and C-14 and from  $CH_2$ -14 to C-2. The planar structure of **1** was thus established as shown in Figure 1.

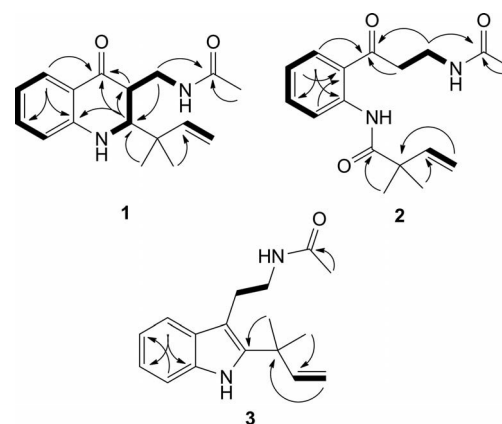


Figure 2. Key COSY (bold line) and HMBC (arrow) correlations of **1–3**.

Compound **1** has two chirality centers, implying four possible stereoisomers, the number of which can be reduced to two by determining the relative configuration. The 2-H and 3-H protons showed a small  $^3J_{H,H}$  coupling constant

Table 1.  $^1H$  and  $^{13}C$  NMR data (500 and 125 MHz, resp.) of **1–3**. Assignments were corroborated by 2D NMR spectroscopy.

Position	<b>1</b> (measured in $[D_6]$ acetone)		<b>2</b> (measured in $CDCl_3$ )		<b>3</b> (measured in $CDCl_3$ )	
	$\delta_H$ (mult., $J$ in Hz)	$\delta_C$	$\delta_H$ (mult., $J$ in Hz)	$\delta_C$	$\delta_H$ (mult., $J$ in Hz)	$\delta_C$
1–NH	6.24 (br. s)		11.64 (br. s)		7.94 (br. s)	
2	3.32 (d, 3.9)	60.9		175.9		140.3
3	2.80 (ddd, 7.6, 6.5, 3.9)	46.8	3.26 (t, 5.8)	39.5	3.08 (t, 7.0)	25.2
4		193.4		203.3		108.1
4a		116.4		121.8		129.9
5	7.53 (d, 7.8)	126.4	7.87 (d, 8.2)	130.7	7.57 (d, 7.4)	118.4
6	6.51 (t, 7.8)	115.4	7.09 (t, 8.2)	122.4	7.11 (t, 7.4)	119.6
7	7.24 (t, 7.8)	135.0	7.54 (t, 8.2)	135.2	7.16 (t, 7.4)	121.7
8	6.81 (d, 7.8)	114.3	8.75 (d, 8.2)	121.0	7.32 (d, 7.4)	110.7
8a		150.5		141.1		134.3
9		42.9		46.8		39.2
10	5.74 (dd, 17.5, 10.8)	144.8	6.13 (dd, 17.3, 10.6)	142.6	6.14 (dd, 17.6, 10.4)	146.1
11	4.95 (d, 17.5)	112.5	5.32 (d, 17.3)	114.6	5.18 (d, 10.4)	112.3
	4.93 (d, 10.8)		5.29 (d, 10.6)		5.17 (d, 17.6)	
12	1.01 (s)	23.8	1.42 (s)	24.7	1.57 (s)	28.0
13	0.95 (s)	22.3	1.42 (s)	24.7	1.57 (s)	28.0
14	3.47 (dd, 13.5, 7.6)	41.4	3.63 (t, 5.8)	34.6	3.55 (t, 7.0)	40.6
	3.21 (dd, 13.5, 6.5)					
15–NH	7.17 (br. s)		6.10 (br. s)		5.59 (br. s)	
16		169.2		170.1		170.4
17	1.87 (s)	21.9	1.96 (s)	23.3	1.93 (s)	23.5

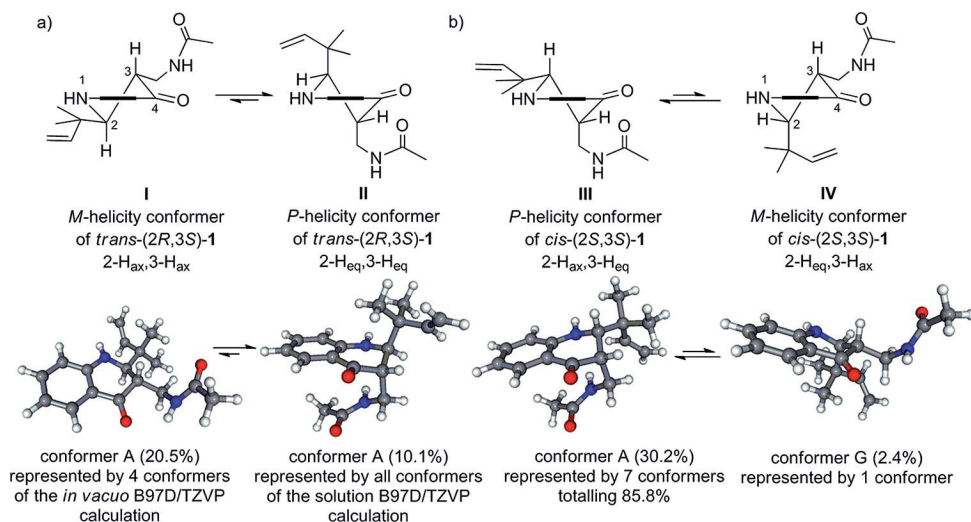


Figure 3. (a) Equilibrating *P*- and *M*-helicity conformers of *trans*-(2*R*,3*S*)-**1** as viewed from the direction of the fused benzene ring (upper) and as obtained by gas phase B3LYP/6-31G(d) and solution (PCM model for acetonitrile) B97D/TZVP conformational analysis (lower). (b) Equilibrating *P*- and *M*-helicity conformers of *cis*-(2*S*,3*S*)-**1** as viewed from the direction of the fused benzene ring (upper) and as obtained by solution (PCM model for acetonitrile) B97D/TZVP conformational analysis (lower).

106 ( $^3J_{2H,3H} = 3.9$  Hz), and an NOE correlation, whereas other  
 NOEs such as correlation of 2-H with 9-Me and 10-H were  
 not of much use to assign the relative configuration. The  
 observed NMR spectroscopic data could derive from either  
 111 *trans*-(2*R*<sup>\*</sup>,3*S*<sup>\*</sup>)-**1**, with diequatorial arrangement of 2-H  
 and 3-H (structure II, Figure 3), or *cis*-(2*S*<sup>\*</sup>,3*S*<sup>\*</sup>)-**1**, with  
 equatorial and axial orientation of the two methine protons  
 (structure III and IV). Thus the relative configuration could  
 not be determined unambiguously on the basis of the  $^3J_{H,H}$   
 and NOE data. For the configurational assignment of **1**,  
 116 conformational analysis of the arbitrarily chosen *trans*-  
 (2*R*,3*S*)-**1** and *cis*-(2*S*,3*S*)-**1** in the gas phase and with polar-  
 izable continuum model (PCM) for acetonitrile and their  
 TDDFT-ECD calculations were therefore carried out. This  
 approach allowed the relative configuration of **1** to be deter-  
 121 mined as *trans*, and the absolute configuration as (2*S*,3*R*).  
 Because in the late stage of our stereochemical study, the  
 relative configuration of **1** was also determined unambigu-  
 ously by X-ray diffraction analysis, details of the conforma-  
 tional analysis and TDDFT-ECD calculation of *cis*-  
 126 (2*S*,3*S*)-**1**, performed to identify the relative configuration  
 by ECD study, is presented only in the Supporting Informa-  
 tion (Figures S1–S4). With the configuration established  
 by X-ray analysis, this part of the investigation may be  
 131 viewed as a case study in determining the relative configura-  
 tion and preferred conformation by ECD analysis for a rela-  
 tively simple molecule, the NMR analysis of which was  
 not suitable for that purpose independently.

The gas-phase B3LYP/6-31G(d) reoptimization of the  
 initial MMFF conformers of *trans*-(2*R*,3*S*)-**1** afforded nine  
 136 conformers above 2% population (Figure S5). The two low-  
 est-energy conformers (20.5 and 16.6% populations) had a  
 hetero-ring of *M*-helicity with *axial* 2-H and 3-H (struc-  
 ture I in Figure 3). The *M*-helicity form had a total popula-  
 tion of 47.0% represented by four conformers. The *P*-helic-  
 141 ity form with *equatorial* 2-H and 3-H (structure II in Fig-

ure 3) had a comparable 36.2% overall population deriving  
 from four conformers, which differed in the orientation of  
 the C-2 and C-3 substituents. The ECD spectrum of **1** in  
 acetonitrile showed a broad intense positive Cotton effect  
 146 (CE) at 384 nm, negative CEs below 323 and 240 nm, and  
 positive CEs at 213 nm and below 205 nm (see Exp. Sec-  
 tion). The B3LYP/TZVP computed ECD spectra of the *P*-  
 helicity conformers (e.g., conformer C) gave an intense  
 long-wavelength CE corresponding to the 384 nm experi-  
 151 mental ECD band (Figure 4), whereas the *M*-helicity con-  
 formers (e.g., conformer A) showed completely different  
 ECD curves. The Boltzmann-weighted computed ECD  
 spectra of the gas-phase B3LYP/6-31G(d) conformers of  
 156 *trans*-(2*R*,3*S*)-**1** showed a mirror image curve of the experi-  
 mental ECD spectrum with acceptable agreement with the  
 tested three methods (B3LYP/TZVP shown in Figure 4).

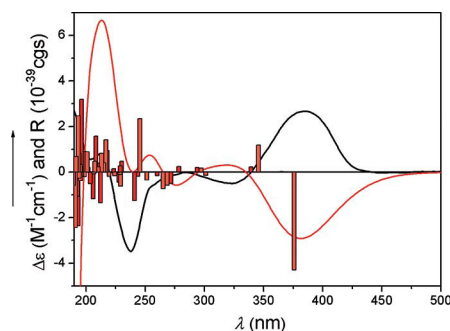


Figure 4. Solution ECD spectrum of **1** in acetonitrile (black) compared with the Boltzmann-weighted B3LYP/TZVP (red, average of nine conformers) computed ECD spectra of the gas-phase B3LYP/6-31G(d) conformers of *trans*-(2*R*,3*S*)-**1**. Rotational strengths of conformer A (*M*-helicity, red bars) and C (*P*-helicity, orange bar) are shown to emphasize differences in their ECD spectra.

The conformational analysis of *trans*-(2*R*,3*S*)-**1** was re-  
 peated at the B97D/TZVP level with the PCM model for

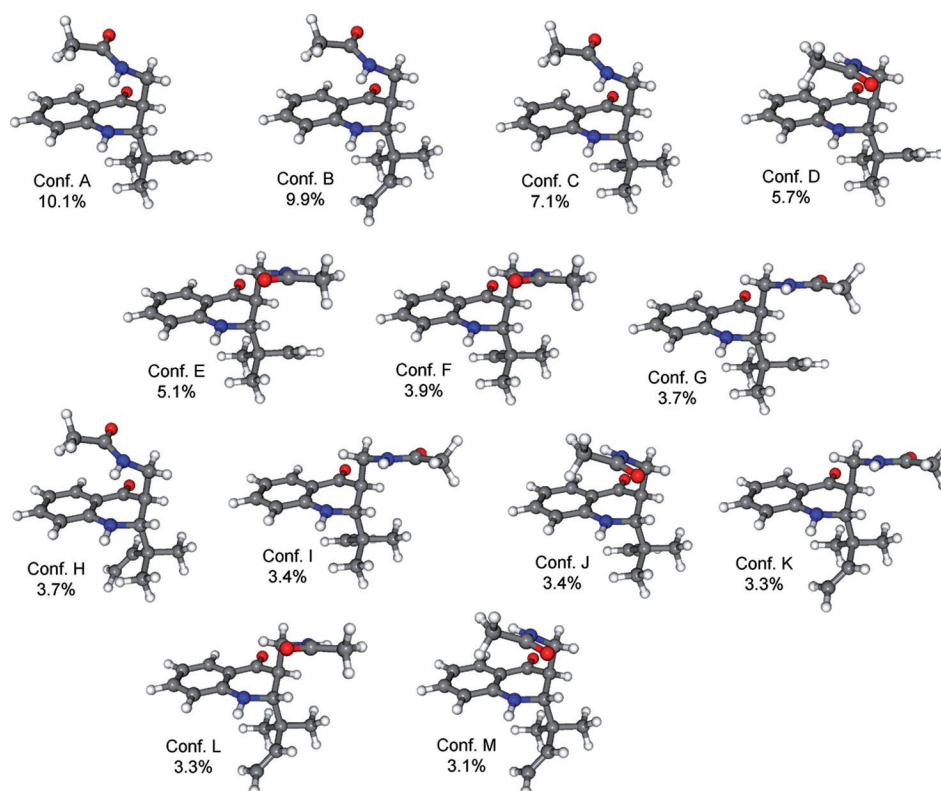


Figure 5. Structures and populations of conformers obtained by B97D/TZVP reoptimization with PCM solvent model for acetonitrile of the initial MMFF conformers of *trans*-(2*R*,3*S*)-**1** above 2% population.

acetonitrile, which resulted in 13 conformers (65.7% total population above 2%) corresponding to the *P*-helicity form with *equatorial* 2-H and 3-H (structure II in Figure 3). In all the conformers, the hetero-ring adopted a half-chair conformation, which is indicated by the similar values of the torsion angles  $\omega_{C-4a,C-8a,N-1,C-2}$  and  $\omega_{C-8a,C-4a,C-4,C-3}$  ( $-14.2^\circ$  and  $-12.1^\circ$ , respectively for conformer A). All the conformers had *P*-helicity and they differed in the rotation of the atoms or groups of the C-2 and C-3 substituents. In contrast to the gas-phase calculation, and in accordance with the NMR spectroscopic data, this method clearly predicted the prevalence of the 2- $H_{eq}$ , 3- $H_{eq}$  conformer (Figure 5), which is attributed to the presence of the bulky 2-methylbut-3-en-2-yl substituent. The computed ECD spectra of the B97D/TZVP solution conformers of *trans*-(2*R*,3*S*)-**1** were consistently mirror image of the experimental ECD spectrum with the three tested methods (B3LYP/TZVP shown in Figure 6). This proved that the absolute configuration of **1** is (2*S*,3*R*) and it was named brocaeloid A.

The 2,3-dihydroquinoline-4(1*H*)-one chromophore of brocaeloid A (**1**) belongs to a group of cyclic aryl ketones that includes the chromane-4-one chromophore in flavanones,<sup>[8]</sup> 2-hydroxyflavanones,<sup>[8]</sup> 2-alkylchromanones,<sup>[9]</sup> and isoflavanones (Figure 7).<sup>[10,11]</sup> The sign of the high-wavelength  $n-\pi^*$  CE of the latter was correlated with the helicity of their hetero-ring by helicity rules, according to which *P*-helicity of the hetero-ring adopting envelope or half-chair conformation is manifested in a positive  $n-\pi^*$  CE

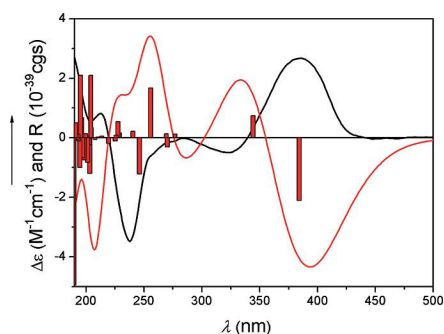


Figure 6. Solution ECD spectrum of **1** in acetonitrile (black) compared with the Boltzmann-weighted B3LYP/TZVP (red, average of 13 conformers) computed ECD spectra of the B97D/TZVP solution conformers of *trans*-(2*R*,3*S*)-**1**. Bars represent computed rotational strengths of conformer A.

above 300 nm.<sup>[12]</sup> Because the 2,3-dihydroquinoline-4(1*H*)-one chromophore is the nitrogen analogue of the chromane-4-one chromophore, a similar helicity rule is expected between the sign of the  $n-\pi^*$  CE and the helicity of the heteroring of the dihydroquinoline-4(1*H*)-one moiety. Our conformational analysis revealed that the hetero-ring of brocaeloid A has half-chair conformation with *M* helicity, which should result in negative  $n-\pi^*$  CE. In contrast, the highest-wavelength ECD band of **1** had a positive CE at 384 nm. Analysis of the Kohn–Sham orbitals showed that the 384 nm UV transition is a pure HOMO–LUMO transition of  $\pi-\pi^*$  origin, whereas the  $n-\pi^*$  transition belongs to the

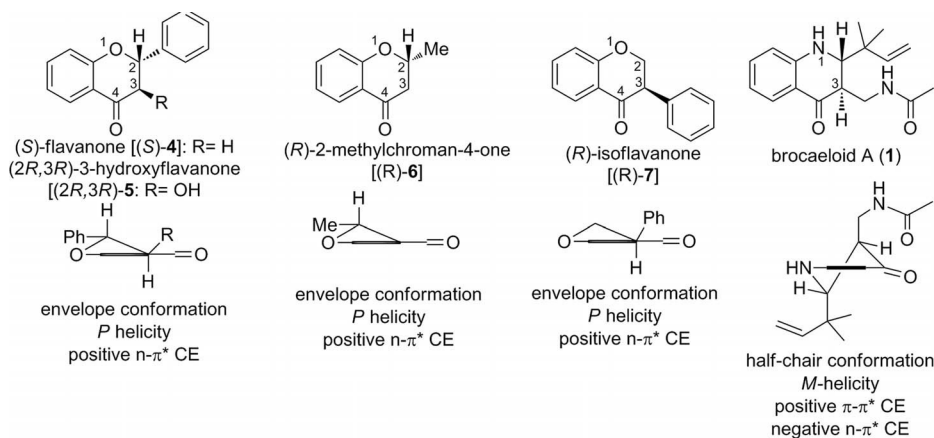


Figure 7. Correlation between the helicity of the hetero-ring in (*S*)-flavanone, (2*R*,3*R*)-3-hydroxyflavanone, (*R*)-2-methylchroman-4-one, (*R*)-isoflavanone, and brocaeloid A (**1**) and the sign of the  $n-\pi^*$  CE.

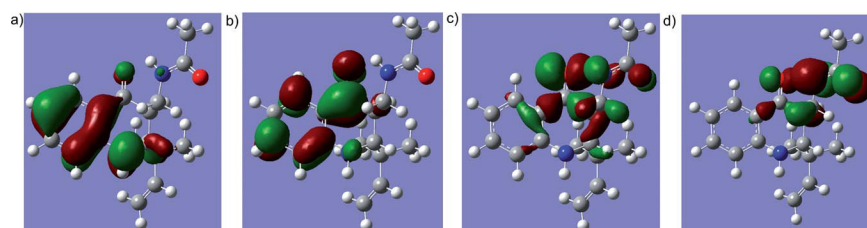


Figure 8. Kohn–Sham orbitals of brocaeloid A (**1**) responsible for the 384 nm  $\pi-\pi^*$  (HOMO→LUMO) and 323 nm  $n-\pi^*$  (HOMO-3→LUMO and HOMO-2→LUMO) transitions extracted from B3LYP/TZVP calculation of the lowest-energy B97D/TZVP (PCM model for acetonitrile) solution conformer and plotted with an isovalue of 0.032: (a) HOMO, (b) LUMO, (c) HOMO-3, and (d) HOMO-2.

201 323 nm band with negative CE (Figure 8). Thus, *M*-helicity of brocaeloid A (**1**) with (2*S*,3*R*) absolute configuration results in a positive  $\pi-\pi^*$  and a negative  $n-\pi^*$  CE, which parallels the helicity rule of the chromane-4-one chromophore.

206 Simultaneously with the ECD calculation studies, crystallization of **1** was performed. Although compound **1** was initially obtained as a light-yellow amorphous solid, after many attempts, single crystals that were suitable for X-ray analysis were obtained by slow evaporation of a solution of **1** in MeOH/CHCl<sub>3</sub> (1:1). The results of the X-ray diffraction analysis confirmed independently that brocaeloid A (**1**) indeed has *trans* relative configuration with *axial* orientation of the C-2 and C-3 substituents (Figure 9).

211 Compound **2**, a colorless oil, was determined to have the molecular formula C<sub>17</sub>H<sub>22</sub>O<sub>3</sub>N<sub>2</sub> on the basis of HRMS (ESI), suggesting eight degrees of unsaturation. The <sup>1</sup>H and <sup>13</sup>C NMR spectroscopic data of **2** (Table 1) were very similar to those of **1**, except that the two methines at  $\delta_C = 60.9$  (C-2) and 46.8 ppm (C-3) of **1** were not present in the spectrum of **2**. Instead, signals for an additional carbonyl at  $\delta_C = 175.9$  ppm (C-2) and a methylene group at  $\delta_C = 39.5$  ppm (C-3) were observed in the NMR spectra of **2**. The above data implied that the hexatomic ring in **1** was opened, and one carbon atom, either C-2 or C-3, was oxygenated to a carbonyl in **2**. The COSY correlation between the nitrogenated methylene (CH<sub>2</sub>-14) and the newly presented methylene (CH<sub>2</sub>-3), as well as the HMBC correlations from the *gem*-dimethyl groups CH<sub>3</sub>-12 and CH<sub>3</sub>-13 to the carbonyl carbon C-2 supported the above deduction,

226

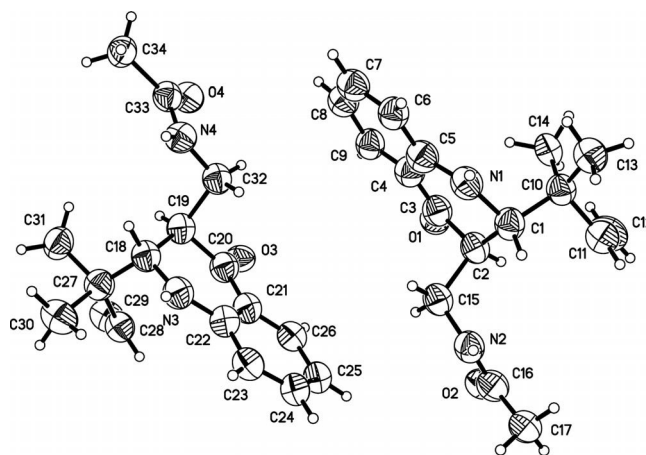


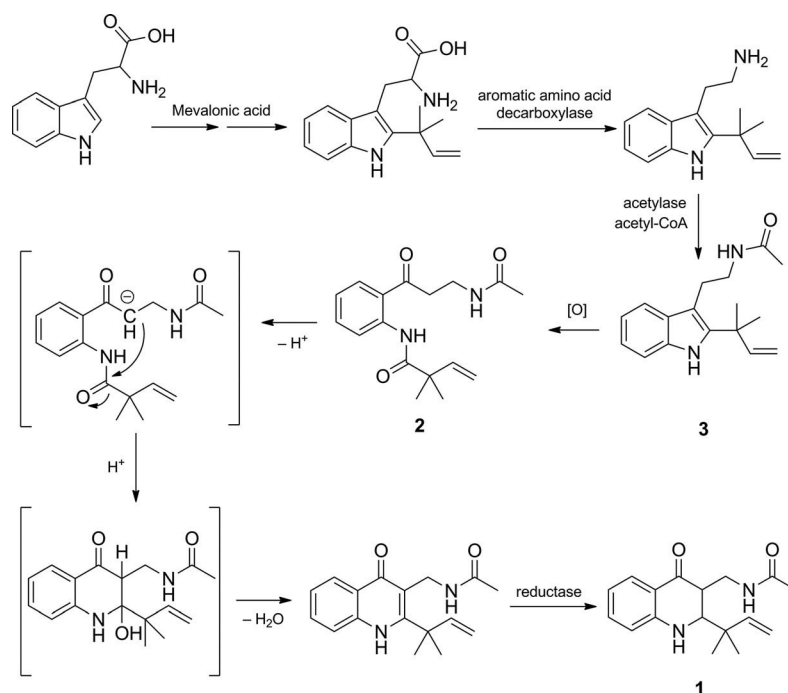
Figure 9. X-ray crystal structure of **1** (a different numbering system is used for the structure in the text).

and the oxygenated C-2 was also established to be a carbonyl carbon. The structure of compound **2** was thus determined and named brocaeloid B.

231

Compound **3** was obtained as a colorless oil and the molecular formula C<sub>17</sub>H<sub>22</sub>ON<sub>2</sub> was determined by analysis of the HRMS (ESI). Detailed comparison of the NMR spectroscopic data of **3** with those of *N*<sub>b</sub>-acetyltryptamine (Figure 1), an indole alkaloid isolated from an unidentified marine algal fungus,<sup>[13]</sup> suggested that they shared similar structure features. However, compound **3** contained an additional isoprenyl substitution at C-2. The significant differ-

236



Scheme 1. Plausible biosynthetic pathways for compounds 1–3.

241 ences in the NMR spectrum of **3** were the absence of an  
 242 olefinic proton signal for 2-H, which was observed at  $\delta_{\text{H}} =$   
 243 7.04 ppm (d,  $J = 2.2$  Hz) in the  $^1\text{H}$  NMR spectrum of *N*<sub>b</sub>-  
 244 acetyltryptamine,<sup>[13]</sup> and the presence of the signals for a  
 245 *trans*-isopentene group (C-9–C-13). The detected HMBC  
 246 correlations from the two *gem*-methyl groups of the isopentene  
 (CH<sub>3</sub>-12 and CH<sub>3</sub>-13) to C-2 verified the prenylation  
 of the indole moiety at C-2. Accordingly, the structure of  
**3** was determined, and the trivial name brocaeloid C was  
 assigned.

251 Compounds containing *N*-acetyl groups were described  
 as naturally occurring microbial secondary metabolites in  
 previous reports.<sup>[13,14]</sup> The close resemblance of compounds  
 1–3 indicated that they are probably generated by a com-  
 252 mon biosynthesis pathway from a tryptophan precursor  
 (Scheme 1).<sup>[15–18]</sup>

253 Compounds 1–3 were evaluated for the lethality against  
 brine shrimp (*Artemia salina*), for DPPH (2,2-diphenyl-1-  
 picrylhydrazyl) radical scavenging potency, and for antibac-  
 254 terial activity against five bacteria. None of these com-  
 255 pounds showed DPPH radical scavenging or antibacterial  
 activity. However, compound **2** exhibited potent lethal ac-  
 256 tivity with an LD<sub>50</sub> value of 36.7 μM, which is more active  
 than that of the positive control colchicine (with LD<sub>50</sub>  
 87.6 μM). The other tested compounds displayed either  
 weak or no activity (LD<sub>50</sub> > 100 μM).

## Conclusions

261 Three new alkaloids, brocaeloids A–C (1–3), containing  
 reversed prenylation in their structures, were isolated from  
 cultures of marine-derived *Penicillium brocae* MA-192. The  
 262 structures of 1–3 were elucidated by analyzing spectroscopic

data generated by 1D and 2D NMR and mass spectrometry.  
 The absolute configuration of brocaeloid A (**1**) was estab-  
 263 lished by the TDDFT-ECD calculation of its *cis*- and  
 264 *trans*-isomers. Calculations showed the importance of con-  
 265 formation in determining relative and absolute configura-  
 266 tion, because **1** exists in solution and solid-state as the  
*trans*-*diaxial* conformer with *M*-helicity due to the steric hin-  
 drance of the C-2 and C-3 substituents. Compound **2**  
 showed lethality against brine shrimp (*Artemia salina*) with  
 an LD<sub>50</sub> value of 36.7 μM.

## Experimental Section

**General:** Optical rotations were determined with an Optical Ac-  
 tivity AA-55 digital polarimeter. UV Spectra were measured with a  
 Lengguang-Gold-Spectrumlab-54 UV/Vis spectrophotometer,  $\lambda_{\text{max}}$   
 (log  $\epsilon$ ) in nm. ECD spectra were recorded with a J-810 spectropola-  
 267 rimeter with a mm ■■■ ((=>Author: x mm?)) ■■■ cell using 1 nm  
 268 bandwidth, 2 s response, standard sensitivity, 100 nm/min scanning  
 speed and 3 accumulations. NMR spectra were recorded with a  
 Bruker–Avance-500 spectrometer (500 MHz for  $^1\text{H}$  and 125 MHz  
 269 for  $^{13}\text{C}$ ),  $\delta$  in ppm,  $J$  in Hz. Low- and high-resolution ESI-MS were  
 270 acquired with a VG-Autospec-3000 mass spectrometer. Semipre-  
 parative HPLC were performed with a Dionex HPLC system  
 equipped with a P680 pump, an ASI-100 automated sample injec-  
 271 tor, and a UVD340U multiple wavelength detector (Sinochrom  
 ODS-BP column, 10 × 300 mm, 10 μm, flow rate 3 mL/min). Col-  
 272 umn chromatography (CC) experiments were accomplished by  
 using commercial silica gel (SiO<sub>2</sub>; 200–300 mesh; Qingdao Haiyang  
 Chemical Group Co.), Lobar LiChroprep RP-18 (40–63 μm;  
 Merck), and Sephadex LH-20 (Pharmacia). TLC analyses were  
 273 performed using precoated SiO<sub>2</sub> GF-254 plates (Qingdao Haiyang  
 Chemical Group Co.). All solvents used for extraction and purifica-  
 274 tion were distilled prior to use.

**Fungal Strain:** The endophytic fungus *Penicillium brocae* MA-192 was isolated from fresh leaves of the marine mangrove plant *Avicennia marina*, which was collected from Hainan island, P. R. China, in August 2012. The fungus was identified by analysis of its ITS region of the rDNA, as described in our previous report.<sup>[19]</sup> The sequence derived from the fungal strain was deposited at GenBank, with accession No. KF513181. A BLAST search result showed that the sequence was the most similar (99%) to the sequence of *Penicillium brocae* (compared to AF484394). The strain is preserved at the Institute of Oceanology, Chinese Academy of Sciences.

**Fermentation:** For chemical investigations, the fungal strain was statically fermented in a 1000-mL Erlenmeyer flask containing 300 mL of the PDB medium (potato dextrose broth: 2% mannitol, 1% glucose, 0.3% peptone, 0.5% yeast extract, and seawater added up to 300 mL, pH 6.5–7.0, adjusted with 10% NaOH/flask, 60 flasks) at room temperature for 30 d.

**Extraction and Isolation:** The mycelium and broth were separated by filtration. The mycelium were homogenized with a waring blender, and the mycelium and broth were exhaustively extracted with EtOAc to give a crude extract (28.0 g), which was dried and fractionated by silica gel vacuum liquid chromatography (VLC) using solvents of increasing polarity from petroleum ether (PE) to MeOH to yield eight fractions (Frs. 1–8) based on TLC analysis. Fr. 6 (6.3 g), eluted with petroleum ether/EtOAc (1:1), was further separated by CC (SiO<sub>2</sub>; CHCl<sub>3</sub>/MeOH, 40:1 to 10:1; Lobar LiChroprep RP-18; MeOH/H<sub>2</sub>O, 3:7 to 0:1; Sephadex LH-20, MeOH), and finally preparative HPLC (MeOH/H<sub>2</sub>O, 55%) to yield **3** (5.0 mg, *t<sub>R</sub>* = 30.51 min). Fr. 7 (3.4 g), eluted with CHCl<sub>3</sub>/MeOH (20:1), was subjected to CC (SiO<sub>2</sub>; CHCl<sub>3</sub>/MeOH, 50:1 to 10:1, then Sephadex LH-20, MeOH) to yield **1** (7.0 mg) and **2** (15.8 mg).

**Brocaeloid A (1):** Yellow prismatic crystals; m.p. 196–197 °C; [*a*]<sub>D</sub><sup>25</sup> = +225 (*c* = 0.20, MeOH). UV (MeOH): 238 (4.20), 262 (3.74), 395 (3.41) nm. ECD [MeCN, *λ* (*Δε*), *c* = 5.83 × 10<sup>-4</sup> M]: 384 (+2.72), 323 (–0.55), 312 sh (–0.47), 273 (–0.21), 260 sh (–0.58), 240 (–3.71), 213 (+1.15) nm; positive below 205 nm. <sup>1</sup>H and <sup>13</sup>C NMR spectroscopic data are presented in Table 1. MS (ESI+): *m/z* = 287 [M + H]<sup>+</sup>. HRMS (ESI): *m/z* calcd. for C<sub>17</sub>H<sub>23</sub>O<sub>2</sub>N<sub>2</sub> [M + H]<sup>+</sup> 287.1754; found 287.1755.

**Brocaeloid B (2):** Colorless oil. UV (MeOH): 231 (4.26), 260 (3.86), 323 (3.48) nm. <sup>1</sup>H and <sup>13</sup>C NMR spectroscopic data are presented in Table 1. MS (ESI+): *m/z* = 303 [M + H]<sup>+</sup>. HRMS (ESI): *m/z* calcd. for C<sub>17</sub>H<sub>23</sub>O<sub>3</sub>N<sub>2</sub> [M + H]<sup>+</sup> 303.1703; found 303.1702.

**Brocaeloid C (3):** Colorless oil. UV (MeOH): 201 (4.36), 224 (4.33), 283 (3.67) nm. <sup>1</sup>H and <sup>13</sup>C NMR spectroscopic data are presented in Table 1. MS (ESI+): *m/z* = 271 [M + H]<sup>+</sup>. HRMS (ESI): *m/z* calcd. for C<sub>17</sub>H<sub>23</sub>ON<sub>2</sub> [M + H]<sup>+</sup> 271.1805; found 271.1811.

**Biological Activity:** The lethality assay against brine shrimp was carried out by a reported method.<sup>[20]</sup> The radical-scavenging activity assay was determined by using the 2,2-diphenyl-1-picrylhydrazyl (DPPH) method.<sup>[21]</sup> The antibacterial assay against *Escherichia coli*, *Staphylococcus aureus*, *Pseudomonas aeruginosa*, *Micrococcus luteus*, and *Vibrio alginolyticus* were carried out by using the well diffusion method.<sup>[22]</sup> Chloramphenicol was used as positive control for the antibacterial assay.

**Computational Section:** Mixed torsional/low mode conformational searches were carried out by means of the MacroModel 9.9.223 software<sup>[23]</sup> using the Merck Molecular Force Field (MMFF) with implicit solvent model for chloroform applying a 21 kJ/mol energy window. Geometry reoptimizations [B3LYP/6-31G(d) level in gas phase and B97D/TZVP<sup>[24,25]</sup> level with PCM solvent model for MeCN] such as TDDFT calculations were performed with

Gaussian 09<sup>[26]</sup> using various functionals (B3LYP, BH&HLYP, PBE0) and TZVP basis set. ECD spectra were generated as the sum of Gaussians<sup>[27]</sup> with 3000 cm<sup>-1</sup> half-height width (corresponding to ca. 31 at 320 nm), using dipole-velocity computed rotational strengths. Boltzmann distributions were estimated from the ZPVE corrected B3LYP/6-31G(d) energies. The MOLEKEL<sup>[28]</sup> software package was used for visualization of the results.

**X-ray Crystallographic Analysis of 1:** Yellow prismatic crystals of **1** were obtained by recrystallization from MeOH/CHCl<sub>3</sub> (1:1). C<sub>17</sub>H<sub>22</sub>N<sub>2</sub>O<sub>2</sub>; *M<sub>r</sub>* = 286.37; monoclinic space group P2(1); unit cell dimensions *a* = 9.5045(6) Å, *b* = 19.4248(16) Å, *c* = 9.6543(9) Å; *V* = 1670.8(2) Å<sup>3</sup>; *a* = *γ* = 90°, *β* = 110.382(2)°; *Z* = 4; *d*<sub>calcd.</sub> = 1.138 mg/m<sup>3</sup>; crystal dimensions 0.38 × 0.10 × 0.07 mm, *μ* = 0.598 mm<sup>-1</sup>; *F*(000) = 616. The 5492 measurements yielded 4012 independent reflections after equivalent data were averaged, and Lorentz and polarization corrections were applied. The final refinement gave *R*<sub>1</sub> = 0.1869 and *wR*<sub>2</sub> = 0.4432 [*I* > 2σ(*I*)]. All crystallographic data<sup>[29]</sup> were collected with a Bruker Smart-1000 CCD diffractometer equipped with graphite-monochromated Cu-*K<sub>α</sub>* radiation (*λ* = 1.54178 Å) at 293(2) K. The data were corrected for absorption by using the program SADABS.<sup>[30]</sup> The structure was solved by direct methods with the SHELXTL software package.<sup>[31]</sup> All non-hydrogen atoms were refined anisotropically. The H atoms were located by geometrical calculations, and their positions and thermal parameters were fixed during the structure refinement. The structure was refined by full-matrix least-squares techniques.<sup>[32]</sup>

**Supporting Information** (see footnote on the first page of this article): Conformational analysis of **1**, solution and computed ECD spectra of **1**, copies of the HRMS (ESI) as well as 1D and 2D NMR spectra of **1–3**.

## Acknowledgments

Financial support by programs from the Ministry of Science and Technology of China (grant numbers 2013AA092901 and 2010CB833800) and from the National Natural Science Foundation of China (NSFC) (grant numbers 31270403 and 30910103914) is gratefully acknowledged. T. K. thanks the Hungarian National Research Foundation (OTKA K105871) for financial support and the National Information Infrastructure Development Institute (NIIFI), 10038 for CPU time.

- [1] J. W. Blunt, B. R. Copp, R. A. Keyzers, M. H. G. Munro, M. R. Prinsep, *Nat. Prod. Rep.* **2012**, *29*, 144–222.
- [2] W. Ebrahim, A. H. Alyl, A. Mándi, F. Totzke, M. H. G. Kubbutat, V. Wray, W. H. Lin, H. F. Dai, P. Proksch, T. Kurtán, A. Debbab, *Eur. J. Org. Chem.* **2012**, 3476–3484.
- [3] D. Liu, X. M. Li, C. S. Li, B. G. Wang, *Helv. Chim. Acta* **2013**, *96*, 437–444.
- [4] D. Liu, X. M. Li, C. S. Li, B. G. Wang, *Helv. Chim. Acta* **2013**, *96*, 1055–1061.
- [5] C. Y. An, X. M. Li, C. S. Li, M. H. Wang, G. M. Xu, B. G. Wang, *Mar. Drugs* **2013**, *11*, 2682–2694.
- [6] Z. Shang, X. M. Li, C. S. Li, B. G. Wang, *Chem. Biodiversity* **2012**, *9*, 1338–1348.
- [7] H. J. Yan, X. M. Li, C. S. Li, B. G. Wang, *Helv. Chim. Acta* **2012**, *95*, 163–168.
- [8] W. Gaffield, *Tetrahedron* **1970**, *26*, 4093–4108.
- [9] W. J. McGahren, G. A. Ellestad, G. O. Morton, M. P. Kunstman, *J. Org. Chem.* **1972**, *37*, 1636–1639.
- [10] D. Slade, D. Ferreira, J. P. J. Marais, *Phytochemistry* **2005**, *66*, 2177–2215.
- [11] C. Galeffi, P. Rasoanaivo, E. Federici, G. Palazzino, M. Nicoletti, B. Rasolondratovo, *Phytochemistry* **1997**, *45*, 189–192.

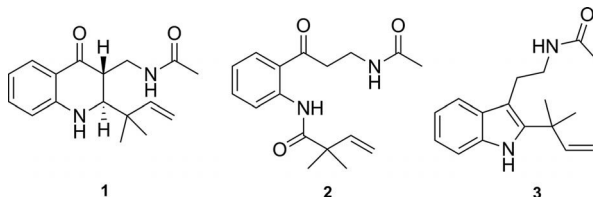
## FULL PAPER

- 426 [12] T. Kurtán, S. Antus, G. Pescitelli, *Electronic CD of benzene*  
and other aromatic chromophores for determination of absolute  
431 configuration in *Comprehensive chiroptical spectroscopy: appli-*  
cations in stereochemical analysis of synthetic compounds, natu-  
ral products, and biomolecules (Eds.: N. Berova, P. L. Polavar-  
apu, K. Nakanishi, R. W. Woody), Hoboken, John Wiley, **2012**,  
vol. 2, p. 73–114.
- [13] Y. Li, X. F. Li, D. S. Kim, H. D. Choi, B. W. Son, *Arch. Pharm-*  
*acol. Res.* **2003**, *26*, 21–23.
- 436 [14] R. N. Asolkar, D. Schröder, R. Heckmann, S. Lang, I. W.  
Döbler, H. Laatsch, *J. Antibiot.* **2004**, *57*, 17–23.
- [15] W. L. Wang, Z. Y. Lu, H. W. Tao, T. J. Zhu, Y. C. Fang, Q. Q.  
Gu, W. M. Zhu, *J. Nat. Prod.* **2007**, *70*, 1558–1564.
- [16] D. R. Hocck, H. G. Floss, *J. Nat. Prod.* **1981**, *44*, 759–762.
- 441 [17] T. A. Wenciewicz, C. T. Walsh, *Biochemistry* **2012**, *51*, 7712–  
7725.
- [18] T. Kametani, N. Kanaya, M. Ihara, *J. Chem. Soc. Perkin Trans.*  
*1* **1981**, 959–963.
- [19] S. Wang, X. M. Li, F. Teuscher, D. L. Li, A. Diesel, R. Ebel,  
P. Proksch, B. G. Wang, *J. Nat. Prod.* **2006**, *69*, 1622–1625.
- 446 [20] M. F. Qiao, N. Y. Ji, X. H. Liu, K. Li, Q. M. Zhu, Q. Z. Xue,  
*Bioorg. Med. Chem. Lett.* **2010**, *20*, 5677–5680.
- [21] K. Li, X. M. Li, J. B. Gloer, B. G. Wang, *Food Chem.* **2012**,  
*135*, 868–872.
- 451 [22] Y. H. Wang, L. Xu, W. M. Ren, D. Zhao, Y. P. Zhu, X. M. Wu,  
*Phytomedicine* **2012**, *19*, 364–368.
- [23] *MacroModel*, Schrödinger LLC, **2012**; <http://www.schrodinger.com/MacroModel>.
- [24] S. Grimme, *J. Comput. Chem.* **2006**, *27*, 1787–1799.
- 456 [25] P. Sun, D. X. Xu, A. Mándi, T. Kurtán, T. J. Li, B. Schulz, W.  
Zhang, *J. Org. Chem.* **2013**, *78*, 7030–7047.
- [26] M. J. Frisch, G. W. Trucks, H. B. Schlegel, G. E. Scuseria,  
M. A. Robb, J. R. Cheeseman, G. Scalmani, V. Barone, B.  
Mennucci, G. A. Petersson, H. Nakatsuji, M. Caricato, X. Li,  
H. P. Hratchian, A. F. Izmaylov, J. Bloino, G. Zheng, J. L. Son-  
nenberg, M. Hada, M. Ehara, K. Toyota, R. Fukuda, J. Hase-  
gawa, M. Ishida, T. Nakajima, Y. Honda, O. Kitao, H. Nakai,  
T. Vreven, J. A. Montgomery, J. E. Peralta Jr., F. Ogliaro, M.  
Bearpark, J. J. Heyd, E. Brothers, K. N. Kudin, V. N. Starov-  
erov, R. Kobayashi, J. Normand, K. Raghavachari, A. Rendell,  
J. C. Burant, S. S. Iyengar, J. Tomasi, M. Cossi, N. Rega, J. M.  
Millam, M. Klene, J. E. Knox, J. B. Cross, V. Bakken, C. Ad-  
amo, J. Jaramillo, R. Gomperts, R. E. Stratmann, O. Yazyev,  
A. J. Austin, R. Cammi, C. Pomelli, J. W. Ochterski, R. L. Mar-  
tin, K. Morokuma, V. G. Zakrzewski, G. A. Voth, P. Salvador,  
J. J. Dannenberg, S. Dapprich, A. D. Daniels, O. Farkas, J. B.  
Foresman, J. V. Ortiz, J. Cioslowski, D. J. Fox, *Gaussian 09*,  
revision B.01, Gaussian, Inc., Wallingford CT, **2010**.
- [27] P. J. Stephens, N. Harada, *Chirality* **2010**, *22*, 229–233.
- [28] U. Varetto, *MOLEKEL*, v. 5.4, Swiss National Supercomput-  
ing Centre, Manno, Switzerland, **2009**.
- 476 [29] CCDC-980111 for **1** contains the supplementary crystallo-  
graphic data for this paper. These data can be obtained free of  
charge from The Cambridge Crystallographic Data Centre via  
[www.ccdc.cam.ac.uk/data\\_request/cif](http://www.ccdc.cam.ac.uk/data_request/cif).
- [30] G. M. Sheldrick, *SADABS*, University of Göttingen, Germany, **481**  
**1996**.
- [31] G. M. Sheldrick, *SHELXTL*, Bruker Analytical X-ray System  
Inc., Madison, WI, **1997**.
- [32] G. M. Sheldrick, *SHELXL-97* and *SHELXS-97*, University of  
Göttingen, Germany, **1997**.
- 486

Received: January 15, 2014




491



496 Brocaeloids A–C (**1–3**), having reversed  
 501 prenylation in their structures, were iso-  
 lated from the mangrove-derived endo-  
 phytic fungus *Penicillium brocae*, and their  
 structures were determined by NMR and

HRMS analysis. The absolute configura-  
 tion of **1** was established, and the results  
 revealed the importance of the confor-  
 mation of the hetero-ring in determining  
 the relative and absolute configuration.

P. Zhang, L.-H. Meng, A. Mándi,  
 T. Kurtán,\* X.-M. Li, Y. Liu, X. Li,  
 C.-S. Li, B.-G. Wang\* ..... 1–9

Brocaeloids A–C, 4-Oxoquinoline and In-  
 dole Alkaloids with C-2 Reversed Prenyl-  
 ation from the Mangrove-Derived Endo-  
 phytic Fungus *Penicillium brocae* 

**Keywords:** Natural products / Alkaloids /  
 Circular dichroism / Density functional cal-  
 culations